Fabrication of Graphitic Carbon Nitride (g-C₃N₄) Photocatalyst and Its Metal-free Efficient Nanocomposites

[1]Arslan Bashir, [2]Muhammadali Raza, [3]Maria Khalid, [4]Urooj Shahzadi

Abstract: **Graphitic carbon nitride (g-C₃N₄) is a group of carbon nitride compounds with a general formula close to C₃N₄ (though commonly with non-zero quantity of hydrogen) and two important substructures dependent on heptazine and poly (Triazine imide) units which liable upon reaction conditions, display reactivities, properties and degree of condensation. Graphitic carbon nitride has high thermal stability, stable chemical structure, non-dangerous nature and medium band gap, as an interesting unique light dynamic semiconductor photocatalyst. This review exhibits the most recent advancement in formation of graphitic carbon nitride C₃N₄. Fused nanocomposites were used to investigate the photocatalytic ability for purification of water. The graphitic carbon nitride based nanocomposites were sorted as non-metal doped g-C₃N₄, noble metals/g-C₃N₄ heterojunction, transition and post transition metal based g-C₃N₄ nanocomposite and g-C₃N₄ without metal nanocomposite. Recently, Graphite carbon nitride (g-C3N4) has gained worldwide attention due to great redox ability, metal free nature, suitable energyd gap and visible response, Graphite carbon nitride (g-C₃N₄) is more energy efficient than TiO₂ and has better photocatalytic ability through solar irradiation because it can absorb visible light directly. Small surface area, insufficient light absorption and fast recombination of hole pairs and photogenerated electron are some drawbacks of pure g-C₃N₄.**

Keywords: **Graphitic carbon nitride (g-C₃N₄), Nanocomposites, advance oxidation process, Waste water treatment, Photocatalysis.**

1. INTRODUCTION

In a time of fast development of material science and science Limin melody and Shujuan Zhang combination the blend of two rising sciences. Limin song began his work in Polytechnic University. They started investigation on Graphitic C₃N₄ photocatalyst for Esterification of benzaldehyde and alcohol under visible light radiation. Aimed their examination they found that the reaction of alcohols and carboxylic acids catalyzed by acids is the customary strategy used to get ready esters in the chemical industry[1].

In this investigation, they report the synthesis of active graphitic carbon nitride (g-C₃N₄) that might be utilized in the one-step reaction between benzaldehyde and alcohol to advance the specific development of esters under visible light illumination. Other than Junying Liu also begun work on graphitic carbon nitride (g-C₃N₄)[2]. He began his work in Jiao Tong University on Efficient photocatalytic hydrogen evolution on N-deficient g-C₃N₄ achieved by a molten salt post-treatment approach. He saw that the carbon nitride (g-C3N4) is a fascinating metal-free photocatalyst for active solar hydrogen production. This disclosure may open a novel avenue to manufactured exceedingly proficient g-C₃N₄ catalysts[3].

Carbon nitride is made out of C and N with some pollution of H, which all is abundant crude materials. Semi-conducting properties of g-C₃N₄ likewise definitely recognize it from graphene[4]. The thermal and chemical stability of g-C₃N₄ in an aqueous suspension stage and under photocatalytic reaction condition makes it an remarkable material[4-5]. This g-C₃N₄ is viewed as the most seasoned engineered polymer previously announced by Berzelius and Liebig in the year 1834 and named as 'melon'[6]. A flow sheet outline is given in (Fig. 1) showing a summary of historic improvement in understanding g-C₃N₄ and its application in photocatalysis. In 1922, Franklin found the exact synthesis of 'melon' to be

C_3N_4. Next, Pauling and Sturdivant determined tri-s-triazine type structure of C_3N_4 in the year 1937[7]. By 1940 it was realized that this material 'melon' has a graphite structure as detailed by Redemann and Lucas. Photocatalysis got huge consideration received after Fujishima and Honda announced photocatalysis of water on TiO_2 in 1972[1]..
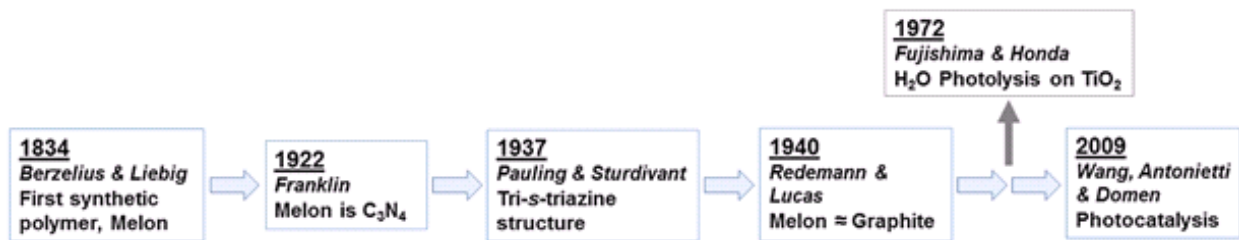
Fig.1. Historic development on understanding g-C_3N_4 and photocatalysis over it[8]

In excess of 5500 research article investigating photocatalytic activity of graphitic carbon nitride were distributed till March 2018 with high significance and huge research premium (Fig. 2).
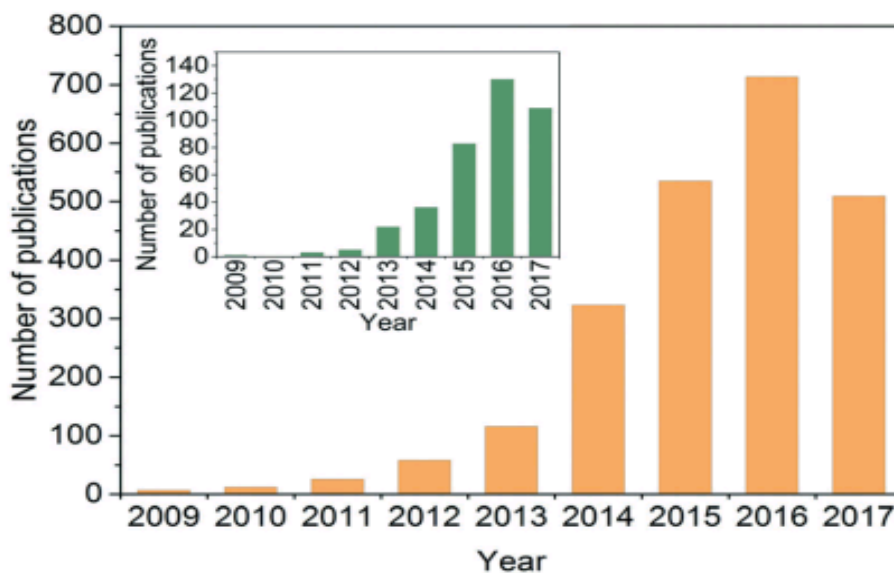
Fig.2. Annual publication details of g-C_3N_4 applications from 1994 to 2018

Wide assortments of materials, for the most part inorganic semiconductors were assesed for photocatalytic application. Graphitic carbon nitride (g-C_3N_4) is a group of carbon nitride compounds with a general formula close to C_3N_4 (through normally with non-zero amount of hydrogen) and two major substructures dependent on heptazine and poly (Triazine imide) units which, contingent on reaction conditions, display various degrees of condensation, properties and reactivities[9]. Novel nonmental catalysts, such as graphitic carbon nitride (g-C_3N_4), have pulled in the consideration of many researchers because of extraordinary their semiconductor properties (band gap of 2.7 eV), visible light absorption, high strength, nontoxicity, and simplicity of planning in aqueous solution. Specifically, the utilization of g-C_3N_4 in photocatalysis has been widely considered. As a photocatalyst, the primary utilization of g-C_3N_4 includes photocatalysis of water to obtain hydrogen, light degradation of organic dyes, and photocatalytic organic reactions. Numerous investigation on the use of photocatalytic oxidation to synthesize organic matter have been performed by Wang and Antonietti, including examines on oxidation of benzene to phenol, oxidation of aliphatic C-H bonds, oxidative coupling of amines, and particular oxidation of alcohols[6].

In recent times, g-C_3N_4 has arisen as the oldest polymer with general formula of $(C_3N_3H)_n$. In year 1990s, Liu and Cohen forecast research of ultra-hard carbon nitride material with diamond like potential. Wang and coworkers investigated photocatalytic action of g-C_3N_4 as metal-free and conjugated stable material for water splitting in 2009. The exclusive properties of g-C_3N_4 like engaging electronic structure, n-type semiconductor, non-poisonous, earth plentiful and adjusted band gap make it reasonable contender for visible light helped photocatalytic water sanitization (Fig. 3)
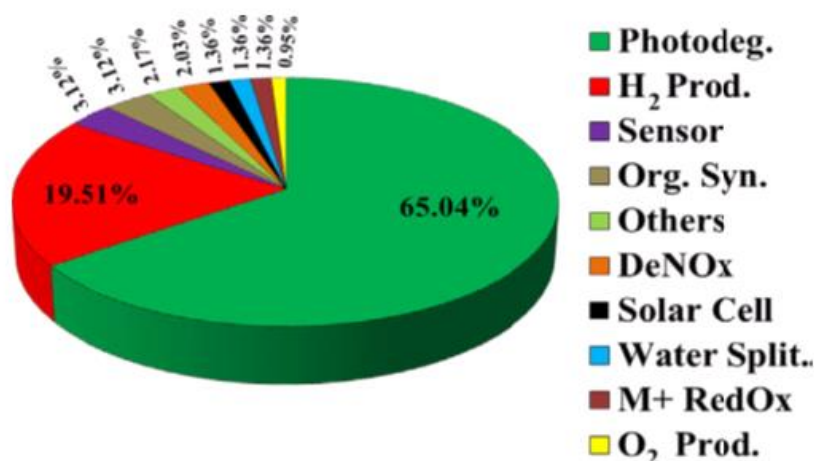
Fig. 3. Pie chart highlighting diverse photoactive applications of g-C_3N_4

Graphitic carbon nitride based photocatalyst comprise one dimensional (1D)[10], two dimensional (2D) nanosheets and three dimensional (3D) categorized structures, widely investigated amid past years with sunlight based vitality use, capable charge transporter partition, improved surface area and uncovered reactive sites[11]. Its chemical resistance is high due to Van der Waals forces among its layer stacking[12]. It is insoluble in toluene, diethyl ether, water, ethanol and THF. Single and few layered g-C_3N_4 is gotten by breakdown of these weak forces. The past reports affirmed flake structured g-C_3N_4 practically identical with graphite[13].

At the start, both hepta-triazine and tri-s-triazine ring were reflected as its tectonic units of g-C_3N_4. On the other hand, later on tri-s-triazine appeared in type of more noteworthy stable structural units associated with planar amino groups[14]. The layered 2D structure of g-C_3N_4 is developed by tri-s-triazine unit. N-type nature and tunable band gap of graphitic carbon nitride with least unoccupied molecular orbital (LUMO) and highest occupied molecular orbital (HOMO) administer its photoelectronic activity[15]. The g-C_3N_4 contains earth-rich components C and N with some substance of H[16]. Semiconductor nature of g-C_3N_4 recognizes it from graphene and different analogues. Along these lines for photocatalytic organic toxin annihilation from water, g-C_3N_4 integrated nanocomposites are viewed as a potential photocatalyst. The g-C_3N_4 pertain yellow shading because of optical absorption at 460nm[16-17]. Various review articles can be followed that centered on synthesis, alteration and catalytic uses of g-C_3N_4 in the field of water decontamination (Fig. 4)[18].
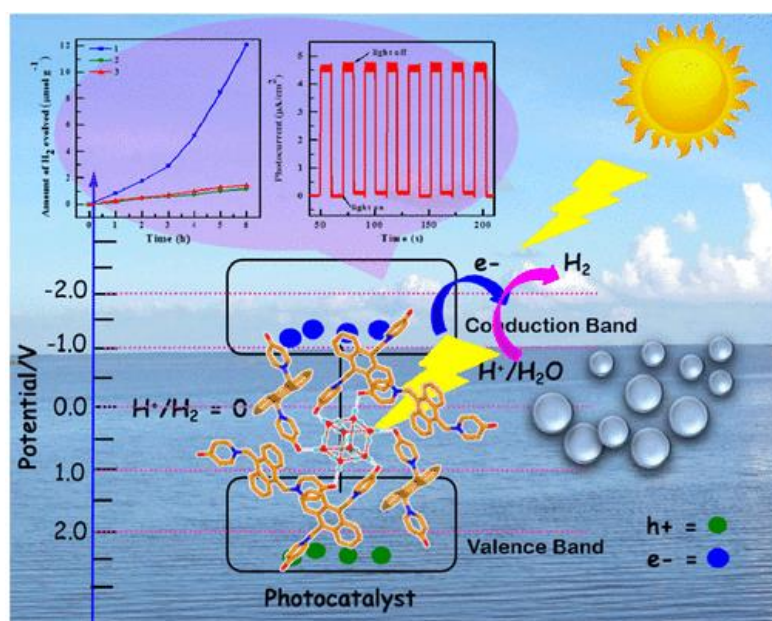
Fig.4. Mechanisitic view of metal free g-C_3N_4 photocatalyst for the degradation of organic pollutants present in water

2. ELECTRONIC STRUCTURE OF g-C$_3$N$_4$

These days, g-C$_3$N$_4$ is viewed as another age photocatalyst to improve the photocatalytic activity of conventional photocatalyst like TiO$_2$, ZnO, WO$_3$ and so on. g-C$_3$N$_4$ should have graphitic like structure[19]. On the other hand, ground state structure of g-C$_3$N$_4$ is as yet not clear and elucidation of accurate ground state structure remains a test for scientists. In the main, thermal polycondensation technique is utilizd to get g-C$_3$N$_4$ and X-beam diffraction technique is connected to explore the crystal structure of g-C$_3$N$_4$[12]. Anyway two temperature dependent X-ray diffraction (XRD) peaks at 2θ=13.04˚ and 27.25˚ just given insufficient data due to low crystallinity of g-C$_3$N$_4$[17]. Scientists trust that these two peaks relate to an in-plane collation with a repeated distance of 3.273Å, individually. Though, exact stacking positions of C and N atoms regarding the neighboring layers are as yet not due experimental confines, and further examination is expected to clear up the stacking order and geometry of g-C$_3$N$_4$[20]. The demand of phase strength was essential, secondary and tertiary. As opposed to other layered structures, mutilated stages in heptazine-based g-C$_3$N$_4$ were the most stable[21]. The stage 1 had direct band gap of 2.87eV and while 2 and 3 phase had indirect band gap of 3.14 and 2.27eV, separately (Fig. 5)[22].

Other research assemblies additionally investigated of g-C$_3$N$_4$, hypothetically. In g-C$_3$N$_4$, lone pair electrons of nitrogen are primarily responsible for ban structure and development of valence band. Abd EI-Kader et al[23]. Moreover, gave related view about concerning result of nitrogen content on optical properties of g-C$_3$N$_4$ to certain degree[24]. Fundamentally, C$_3$N$_4$ is available in seven stages for example a-C$_3$N$_4$, b-C$_3$N$_4$, cubic C$_3$N$_4$, pseudocubic C$_3$N$_4$, g-h-triazine, g-o-triazine and g-h-heptazine with band gaps of 5.49, 4.85, 4.30, 4.13, 2.97, 0.93 and 2.88eV, respectively[25].
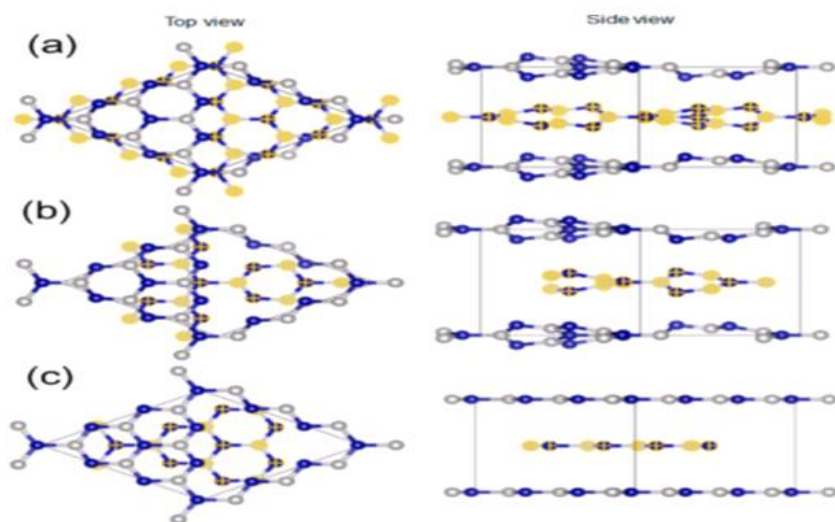
Fig.5. Predicted images of heptazine-based g-C$_3$N$_4$, (a) predicted most stable configuration, phase 1, (b) second stable distorted configuration, phase 2, (c) most stable planar configuration, phase3. The atoms in the middle layer of the lattices are labeled with yellow crosses. (With permission from ACS-Applied materials and interface) (For interpretation of the references to color in this figure legend

The different allotropes of g-C$_3$N$_4$ were shaped by triazine (C$_3$N$_4$) and tris-triazine/ heptazine (C$_6$N$_7$) rings unit. Tri-s-triazine based g-C$_3$N$_4$ is viewed as most stable period of g-C$_3$N$_4$. Pseudocubic and g-h-triazine phases of g-C$_3$N$_4$ have direct band gaps and all various phases have indirect band gaps[26]. The reduction and oxidation potentials are associated with positioning of valence and conduction band as for standard reduction potential scale of hydrogen. Kroke et al. used functional theory (DFT) calculations to investigate electronic structure of g-C$_3$N$_4$[27]. The optical band gap of melon was 2.6eV that reduced from 3.5eV of melem and lastly accomplished the value of 2.1eV with complete formation of condensed g-C$_3$N$_4$[28]. The wave function examination investigated that valence and conduction band are fundamentally directed by nitrogen (N) P$_Z$ orbitals and carbon (C) P$_Z$ orbitals, respectively[26, 29]. The EHP partition proposes free oxidation and reduction sites for water splitting in nitrogen and carbon atom. Wei and colleagues utilized many body Green's function technique for examination of electronic and optical properties of g-C$_3$N$_4$[30]. The got outcomes guaranteed that electronic band gap of g-C$_3$N$_4$ was 4.24eV[31]. While, tri-s-triazine based catalyst had 5.22eV (direct) and 4.15eV (indirect) band gaps. In addition, it was affirmed that in electronic structure of g-C$_3$N$_4$ valence and conduction are shaped by overlap of 2p orbital of nitrogen and 2p orbital carbon atom together[32] Decisively, two-dimensional (2D) structure of

Page | 70

g-C_3N_4 can be considered as a nitrogen atom-substituted graphene system having conjugated graphitic planes with sp^2 hybridization of carbon and nitrogen atoms in an atomic ring[30, 33]. The lone pair electron of nitrogen is supposed to form lone pair valence band which is balanced out by stabilized by π electronic state. The mid-way band gap ($\sim$2.7eV) allows it to absorb light over wide range of wavelengths in visible region[34]. While, suitable situating of reduction level of conduction band (-1.3eV) and oxidation level of valence (+1.4eV) band initiates the catalytic reactions[29].

3. PREPARATION OF GRAPHITIC CARBON NITRIDE BASED NANOCOMPOSITE

In recent times, advancement has been seen in improved techniques for preparation of g-C_3N_4 based photocatalysts including relationship between structural /morphological features and there photocatalytic activity[35]. Essentially, top down and bottom up approaches have been approved for production of g-C_3N_4 based photocatalysts[36]. Top down approach includes the systematic and stepwise breaking down of larger blocks of g-C_3N_4 into smaller units, namely, g-C_3N_4 nanosheets and few-layered g-C_3N_4, while "bottom up" method contains the combination of smaller molecules to form bigger complex molecules[37]. All through synthesis of g-C_3N_4 and its composite photocatalyst, previous method has been mostly utilized in liquid and thermal exfoliation approaches[38]. While last methodology mainly involves soft and hard template method, solvothermal method and supramolecular aggregation. Mostly, techniques for preparation of g-C_3N_4 can be categorized [37, 39]as:

3.1 Thermal polymerization method

Graphitic carbon nitride (g-C_3N_4) can be ready by thermal polymerization of oxygen-free and nitrogen-rich compound precursors having bonded core structures (triazine and heptazine derivatives)[28] e.g. urea, melamine, dicyandiamide, cyanamide, thiourea, guanidine thiocyanate, guanidine hydrochloride *etc*. The C and N precursors have basic and effective condensation pathways to form polymeric g-C_3N_4 network[40]. Precursor type and synthesis process can strongly affect physical and chemical properties of g-C_3N_4 and C/N ratio in nanostructures[35]. Polyaddition and polycondensation forms are utilized to shape melamine and to expel ammonia, respectively[41]. Melamine based products are obtain above 350˚C, whereas rearrangements of melamine lead to the formation of tri-s-triazine unit products at approximately 390˚C. Further polycondensation of this unit forms final polymeric g-C_3N_4 product at roughly 520˚C (Fig. 6).

Above 600˚C g-C_3N_4 turn into slightly unstable and heating upto 700˚C causes the development of nitrogen and cyano fragments. For instance, at 550˚C temperature, nitrogen rich forerunner *i.e.* urea can be changed to g-C_3N_4. The last result of g-C_3N_4 is generally yellow colored powders. Solid g-C_3N_4 got after thermal condensation/polymerization of monomers did not have crystalline structure with C/N molar ratio of 0.72:1 and small amount of H. 3D bulk, 2D nanosheets, 2D films, 1D nanorods, 1D nanotubes, 1D nanowires and 0D quantum dot of g-C_3N_4 were attained by introduction of many surface modifications and functionalities. The conduction and valence bands positioning were considered by density function theory (DFT) calculations with an estimate that g-C_3N_4 was mostly composed of nitrogen Pz orbitals and carbon Pz orbitals.
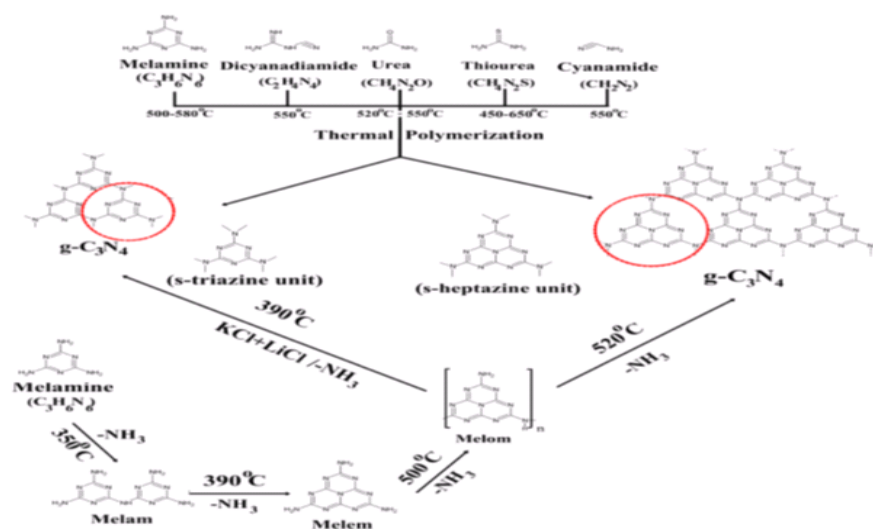
Fig.6. Fabrication of g-C_3N_4 using different precursors.

3.2 Template-assisted methods

In this technique, organic/inorganic molecules are utilized as templates to synthesize porous g-C_3N_4 based photocatalyst. The mesoporous silica and block polymers can be utilized as a layout for the planning of mesoporous carbon including g-C_3N_4. Silica nanoparticles (12nm) utilized as hard template to prepare mesoporous graphitic carbon nitride utilizing thermal condensation cyanamide[23b, 42]. The mesoporous g-C_3N_4 displayed fluctuated surface area from 8 to 373m^2/g. The mesoporous g-C_3N_4 had a band gap of 2.7eV.

The portrayal results describe the controlled surface area of 445-585 m^2/g with a controlled surface area of mesoporousg-C_3N_4. Zheng et al[43]. Reported helical graphitic carbon nitride with twisted hexagonal rod-like morphology using chiral silicon dioxides as template[44]. This helical g-C_3N_4 exhibited C_3N_4 optical and photocatalytic activities for the fabrication of optical devices and asymmetric photocatalysis[45].He used 1-butyl-3-methylimidazolium tetrafluoroborate (BmimBF$_4$) as soft template for the preparation of B and F doped mesoporous graphitic carbon nitride. The mesoporous g-C_3N_4 showed high surface area of 444m^2/g with active sites for catalytic reactions[46].

3.3 Chemical functionalization of g-C_3N_4

Because of 2D nanosheets structure and π conjugated frameworks, graphitic carbon nitride can be utilized to ideal host stage for the manufacture of metal/non-metal nanocomposites utilizing chemical functionalization process[47]. The band gap arrangement between g-C_3N_4 and other semiconductor phtocatalysts arisen as a potential procedure to limit the electron-hole pair recombination during photocatalytic processes[48]. Ag_2CO_2 and g-C_3N_4 based photocatalytic were set up by utilizing in situ precipitation strategy. The Ag^+ ions were in situ precipitated to Ag_2CO_3 by the addition of $NaHCO_3$ and shaped a tight junction between Ag_2CO_3 and $NaHCO_3$. Ag_2CO_3 nanoparticles (5-10nm) were evenly dispersed over g-C_3N_4[49]. The photoluminescence results demonstrated the decrease in recombination rate of photo generated electron hole-pair in Ag_2CO_3/g-C_3N_4 nanocomposite[50].

The decreased recombination rate was because of migration of hole from VB of Ag_2CO_3 to VB of g-C_3N_4 while electrons were removed from CB of g-C_3N_4 to CB of Ag_2CO_3. So as to additionally improve the activity of photocatalytic system, binary photocatalyst have been hybridized with g-C_3N_4 to get ready ternary photocatalyst. To the mixture of Zn $(NO_3)_2.6H_2O$ and In $(NO_3)_3.4H_2O$(Zn/In molar ratio 3.0) were broken up in distilled. 50ml of each NaOH (0.24M) and Na_2CO_3 (0.1M) were added dropwise to get ZnIn-LDH. The ZnIn-LDH was mixed with melamine via grinding process to obtain ZnIn-LDH/g-C_3N_4[51]. The photocatalytic activity of ZnIn-LDH/g-C_3N_4 was assessed the removal of Rhodamine-B dye. The improved surface area and effective charge separation of photogenerated electron hole pair were in charge of improved photocatalytic activity[52]. Huang et al. arranged amine-functionalized g-C_3N_4 by heating urea at 500˚C, with asubsequent functionalization treatment using monoethanolamine solution and effectively exhibited that surface amine functionalization represented itself as an effective approach to enhance CO_2 adsorption capacity of g-C_3N_4. The amine-functionalized g-C_3N_4 demonstrated enhanced photocatalytic performance on CO_2 photoreduction[53].

3.4 Ultrasonication Assisted Exfoliation Method

Encouraged by exfoliation of graphene, ultrasonication assisted liquid exfoliation routes have been broadly utilized for fabrication of g-C_3N_4 and its nanocomposites. Zhang et al. detailed that multilayered g-C_3N_4 can be adequately isolated into few layered 2D sheets utilizing continuous ultrasonication[41]. The exfoliation procedure is greatly influenced by the surface energies of the utilized solvent molecules[54]. The enthalpy of mixing was decreased because of surface energy of g-C_3N_4 flakes when formamide and tetrahydrofuran were utilized as solvent. Ma et al. arranged protonated ultrathin 2D g-C_3N_4 nanosheets from dicynandiamide forerunner utilizing 10M HCl solvent and sonication treatment[55]. So as to keep the agglomeration g-C_3N_4 sheets before heating by heating dicyandiamide at 550˚C. The acquired sheets had 6-12 monolayers of g-C_3N_4 with high dispersion in water. The facile penetration of Li^+ ions into layers of bulk g-C_3N_4 nanosheets advanced the synthesis of better superiority of few layered g-C_3N_4 sheets[56].

3.5 Sol-gel method

Because of high purity and homogeneity of sol-gel strategies are much of time used to manufacture g-C_3N_4 and its nanocomposites[57]. It is considered as one of the reasonable technique because of low cost, ambient processing temperature and easy synthesis route. Fabricated g-C_3N_4-TiO_2 nanocomposite via facile sol-gel method using tetra-n-butyl titanate as precursor, which undergone hydrolysis and polycondensation reaction to form a colloid solution. The characterization results confirmed the intimate contact between g-C_3N_4 to form hetrojunction structures[58]. The sol-gel

Page | 72

conserved as most suitable technique for the formation of $g\text{-}C_3N_4$ and metal oxide semiconductor photocatalyst due to formation of metal –OH network. TiO_2/C_3N_4 nanocomposite exhibited surface area of $140.13 m^2 g^{-1}$[59].

4. GRAPHITIC CARBON NITRIDE BASED METAL-FREE NANOCOMPOSITES

4.1 $C_{60}/g\text{-}C_3N_4$ nanocomposites

Metal-free semiconductors have been given important consideration to solve environmental and energy issues to great potential. Broad research was directed to couple $g\text{-}C_3N_4$ with non-metal/carbonaceous compounds and a portion of these are multi-walled carbon nanotubes (MWNTs)/$g\text{-}C_3N_4$, polypyrrole/C_3N_4, P/C_3N_4, CN/CNS and $C_{60}/g\text{-}C_3N_4$. Fullerene, CNT, graphene and carbon nanodots with π-conjugated structures were viewed as effective supports for photocatalytic nanomaterials to reduce EHP owing to structural, optical properties and electronic features[60]. Numerous research groups have fabricated heterojunctions of $g\text{-}C_3N_4$ with carbonaceous nanomaterials to make increasingly efficient and recyclable photocatalyst for water purification. $C_{60}/g\text{-}C_3N_4$ nanocomposite possessed high visible light absorption due to gray color of $C_{60}/g\text{-}C_3N_4$[61]. Fig. 7 demonstrated mechanism for EHP separation and transportation of electrons at $C_{60}/g\text{-}C_3N_4$ interface. Upon experience to visible light, electrons (e⁻) were excited from VB (occupied by N2p orbitals) to CB (formed by C2p orbitals of $g\text{-}C_3N_4$) leaving behind holes (h⁺) in VB[62].
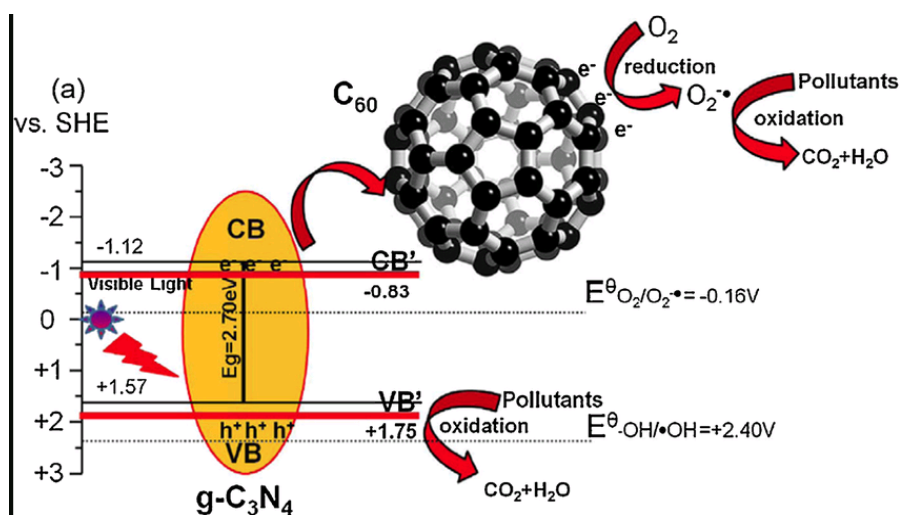
Fig.7. Mechanism of charge separation as well as photocatalytic process of $g\text{-}C_3N_4$ and $C_{60}/g\text{-}C_3N_4$ photocatalyst under visible light irradiation for pollutants degradation.

The photogenerated electrons on CB of $g\text{-}C_3N_4$ were exchanged to C_{60} particles in $C_{60}/g\text{-}C_3N_4$ nanocomposites and advanced EHP separation. Fullerenes (C_{60}) have 30 molecular orbitals with 60 π-electrons with closed-shell configuration leading to effective shuttling and transportation of photogenerated electrons. In view of huge exaction diffusion length and high exciton mobility of C_{60} photogenerated electrons from $g\text{-}C_3N_4$ were instantly transferred on C_{60} to enhance separation of EHP[63]. The separation of EHP caused effective ring benzene opening aimed degradation process and eventually mineralized organic pollutants into inorganic ions.

4.2 CNT/$g\text{-}C_3N_4$ nanocomposite

Carbon nanotube (CNT) is an significant carbon allotrope with excellent conductivity and large specific surface area favoring improved photocatalytic degradation of aqueous phase pollutants[64]. A number of reports guarantee the advantages of coupling of $g\text{-}C_3N_4$ with CNT to fabricate nanocomposite for different photocatalytic energy and environmental applications. Ge and Han coupled MWCNTs with $g\text{-}C_3N_4$ to report CNT/$g\text{-}C_3N_4$ photocatalyst. The improved activity was because of remarkable electron storage ability of CNTs that prohibited past EHP recombination. The coupled CNT/$g\text{-}C_3N_4$ nanomaterial with negative polarity is not easy to prepare due to electrostatic repulsion between CNT and $g\text{-}C_3N_4$. CNT/white $g\text{-}C_3N_4$ nanocomposites were manufactured by treating $g\text{-}C_3N_4$ with HCl accompanied by hydrothermal process based addition of CNT. White $g\text{-}C_3N_4$ acquired polarity of +3.3mV after $g\text{-}C_3N_4$ protonation, favoring coupling with negatively charged CNT. The decrease in zeta potential (+1.6mV) of CNT/$g\text{-}C_3N_4$ compared to white $g\text{-}C_3N_4$ (+3.3mV) was due to interface contact between CNT and $g\text{-}C_3N_4$. The transfer of photogenerated electrons

to CNT and hetero-structure formation between CNT and white g-C_3N_4 played an important role for efficient charge carrier (EHP) separation[65].

4.3 Graphene/g-C_3N_4 nanocomposite

In recent times, two dimensional graphene has involved much consideration due to its outstanding properties e.g. thermal, mechanical, electrical properties, high specific surface area (~2600m^2g^{-1}), marvelous thermal conductivity (~5000$Wm^{-1}K^{-1}$) and mobility of charge carriers (200000$cm^2V^{-1}s^{-1}$)[66]. Subsequently, graphene is regarded as a potential candidate to construct layered graphene and g-C_3N_4 based metal free nanocomposites. Graphene/g-C_3N_4 nanocomposite was organized by means of numerous approaches for photocatalytic degradation of MO under visible-light irradiation[67].

The g-C_3N_4 was embedded between graphene sheets via polymerization of pre-adsorbed melamine molecules on graphene oxide sheets. The compact structure of graphene/g-C_3N_4 led to high photocatalytic activity when electrons (e^-_{CB}) of g-C_3N_4 excited from valence band (VB) to conduction band (CB), fabricating hole (h^+_{VB}) in VB under solar light. The transferred electrons get composed on Pt nanoparticles overloaded on graphene sheets via percolation process[16, 68]. Amid immobilization of g-C_3N_4 on graphene sheets surface, photogenerated electrons on conduction band of g-C_3N_4 had inclination to got exchange on graphene sheets inferable from astounding electronic conductivity of graphene and prevent electron-hole pair recombination to form layered composites. The photocatalytic mechanism including graphene/g-C_3N_4 nanocomposites under visible light is described by Eqs.

graphene /$gC_3N_4 \xrightarrow{hv}$ graphene(e^-) /$gC_3N_4(h^+)$

graphene (e^-) + Pt → graphene + Pt(e^-)

Pt (e^-) + 2H^+ → Pt + H_2

gC_3N_4 (h^+) + CH_3OH + 6OH^- → gC_3N_4 + CO_2 + 5H_2O
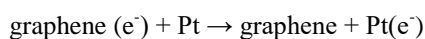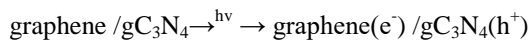
Ternary g-C_3N_4 /graphene /S heterojunction were accounted by immobilizing reduced graphene oxide and g-C_3N_4 sheets on cyclooctasulfur crystal. g-C_3N_4/graphene /S ternary nanocomposite showed important photocatalytic activity for bacterial evacuation under visible light[69].

4.4 Carbon quantum dot /g-C3N4 hybrid nanocomposite

Carbon quantum dots (CQDs) show great properties, for example, outstanding conductivity, being chemical composition and photo-chemical stability. CQDs characterize their different appropriateness in chemical modification and surface passivation with different organic, polymeric, inorganic or biological materials. The forerunners utilized for preparation of both nanomaterials were combined together and heated at 650˚C to get hybrid heterojunction. Carbon nano-particles with 60nm sizes were in situ prepared from a zeolitic imidazolate framework involving thermal polymerization of melamine into g-C_3N_4. The entire composite was treated with HCl solution to remove residual Zn^{2+} before performing photocatalytic activity test[70].CQD modified g-C_3N_4 hybrid was combined using C-dots and dicyandiamide as precursor molecules. CQD resulted in distortion of g-C_3N_4 lattice. CQD/g-C_3N_4 showed improved photocatalytic activity for the degradation Rhodamine dye under UV light. The absorption edge displayed a blue shift compared to bulk g-C_3N_4 and emission peak was shifted towards lower wavelength with decrease in optical band gap. Graphitic carbon nitride nanosheets were altered through heating of bulk graphitic carbon nitride in presence of NH_3. The modified g-C_3N_4 nanosheets had wide band gap of 2.95eV and self-developed carbon vacancies[71]. The permeable nanosheets showed great improvement in photocatalytic proficiency in comparison to bulk g-C_3N_4. The modified g-C_3N_4 nanosheets were very steady under test conditions and photocatalytic activity was 20 times higher as compared to bulk material under visible light.

4.5 g-C_3N_4 /g-C_3N_4 isotype nanocomposite

g-C_3N_4/sulphur doped C_3N_4 (CNS) nanocomposite was manufactured by utilizing a facile surface-assisted polymerization i.e. CNS-CN (CN acting as the host) and CN-CNS (CNS acting as the host)[72].Layered g-C_3N_4 /g-C_3N_4 metal free nanocomposite was produced by using urea and thiourea as precursors to obtain different band structures[73]. TEM images showed effective development of layer between CN-T and CN-U nanosheets. Under visible light , photo-excited electrons were moved from CN-T to CN-U driven by conduction band offset of 0.10eV, while the photo-excited holes drifted from g-C_3N_4 (urea) to g-C_3N_4 (thiourea) due to valence band offset of 0.40eV (Fig. 8).
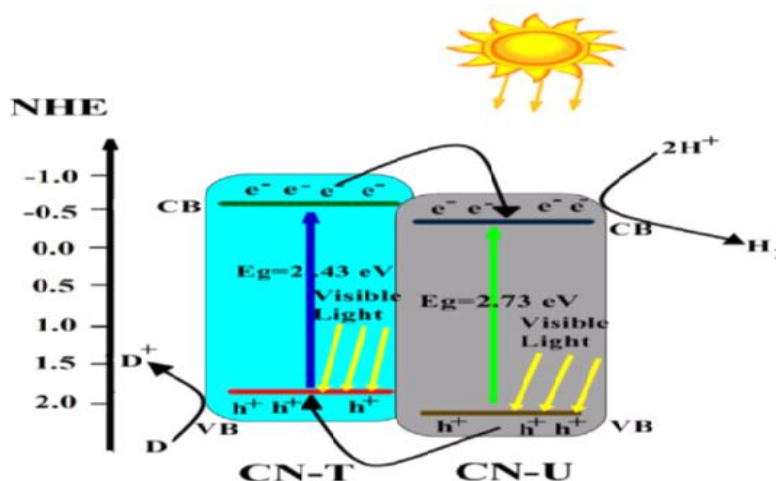
Fig.8. Photocatalytic mechanism illustrating comparison between CN-T (T- Thiourea) and CN-U (Urea)

The addition of electrons on one side of heterojunction (CN-U) as well as holes on other side (CN-T) reduced EHP recombination and prolonged the life time of charge carriers, ensuing high photocatalytic efficacy of the synthesized materials[74].

5. PRACTICAL APPLICATIONS OF g-C$_3$N$_4$ PHOTODEGRADATION

When the different g-C$_3$N$_4$ nanocomposites are used in the useful applications of photocatalysis for waste water treatment, additional consideration should be given to few important working parameters.

5.1 Reusability of g-C$_3$N$_4$ Photocatalysts

All through wastewater treatment at commercial scale, the retrieval and reprocess of the catalyst are important in order to make the procedure competitive. The catalyst of Ag$^{@}$AgCl-g-C$_3$N$_4$ permeable nanosheet is an illustrative example due to relatively high degradation efficacy and the reusability was assessed by reprocessing the photocatalyst for RhB elimination under visible light. Afterward each cycle of photodegradation, the catalyst, Ag$^{@}$AgCl-g-C$_3$N$_4$ permeable nanosheet was centrifuged, washed three times with distilled water, and dried out at 150˚C for 4 h[73]. The consequences (Fig. 9A) display only an insignificant reduction in the degradation rate being detected after eight sequential photocatalysis cycles. As a result this material has not only high photo catalytic capability but also outstanding strength, both of which empower the catalyst to be encouraging visible-light driven catalyst for pollutant elimination. In another study, manufactured a metal-doped catalyst (Na-g-C$_3$N$_4$) which was repetitive for the photodegradation process four times, with no observable reduction in the deprivation rate being observed(Fig.9B)and demonstrating good reusability[73].
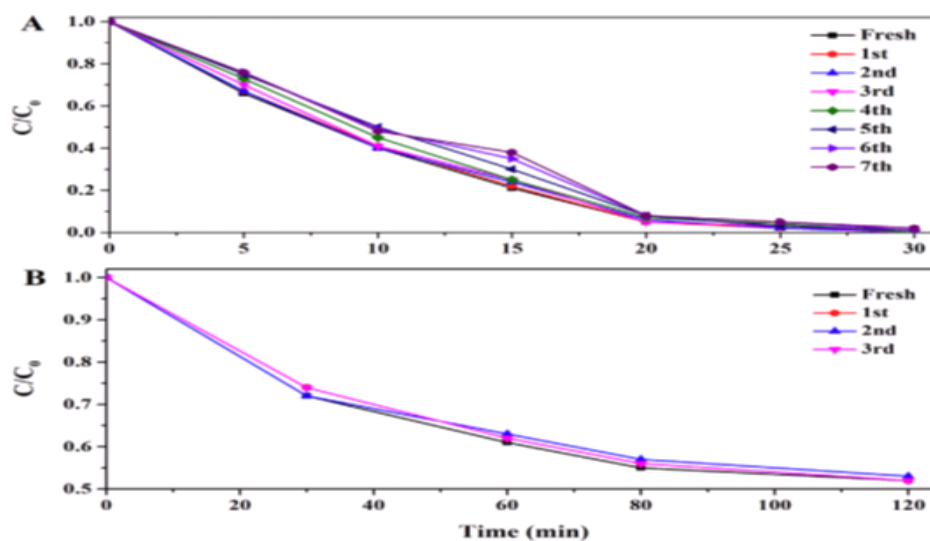
Fig. 9. Recycle tests of (A) Ag$^{@}$AgCl-g-C$_3$N$_4$ porous nanosheets and (B) Na-g-C$_3$N$_4$ under visible light irradiation for RhB removal.

Also, some different components engaged with the pragmatic applications, for example, impetus stacking and the stream rate of wastewater may cause potential effect on the reusability of the impetus. In exploring the photocatalysis by TiO2, Li (2010) announced that 6.0 g L^{-1} of impetus would prompt the most elevated photodegradation rate of COD evacuation while high stream rate negatively affected the corruption adequacy of COD expulsion. Be that as it may, there is an information hole on variables affecting impetus execution among TiO2 and g-C3N4. In this manner, further research is expected to decide the affecting elements for the activity and reusability of combined g-C3N4 in reasonable applications.[69]

5.2 Photocatalytic Reactor for g-C$_3$N$_4$ Nanocomposites

Photocatalytic reactor is intended for the photodegradation of the toxins from water and wastewater. Many reactors have been intended for TiO$_2$ immobilization while few are useful for g-C$_3$N$_4$. Contrasted with the difference of the reactors, g-C$_3$N$_4$ catalyst just need visible light as opposed to UV light which is necessary for TiO$_2$ due to the different absorption ability of light source between the two catalysts[70]. Moreover, unadulterated g-C$_3$N$_4$ catalysts own the non-metal property so the leakage and recycle of the metal should not be a problem for consideration in the reactor. Regularly the photocatalytic tests directed in the research facility utilize a suspension photocatalytic reactor as shown in Fig. 10A, which has the benefits of basic structure, convenient task, frequent compound transmission, and high rate of reaction. However, it additionally has few drawbacks: firstly, the particle size has strong influence on the suspended state of the catalyst, namely, too small size would result in particle deposition. Moreover, the particle size as well affects the light transmission as large size or high concentration would lead to a turbid solution so that the light transmission will be disturbed and light absorption reduced. All the more significantly, the catalysts suspended in the solution are difficult to be isolated and re-used[70].

In this manner, the loaded photocatalytic reactor is desirable to be utilized for g-C$_3$N$_4$ nanocomposite application. As shown in Fig. 10B, g-C$_3$N$_4$ on structured Al$_2$O$_3$ ceramic foam synthesized by Dong et al. (2014a) could be fixed at one side of the reaction pool and the unclean water flows from intake to outlet passing however the loaded g-C$_3$N$_4$ materials[75]. On the other hand, such a reactor structure would definitely produce two problems: one is the restricted reaction area which is just the cross-sectional zone of g-C$_3$N$_4$ on the Al$_2$O$_3$ foam; the other one is comparatively short residence time of contacting the catalyst, which will prompt to the incomplete photodegradation[71]. Therefore, tubes, fibers, and floated glass balls have been planned for the substitution of the single tiled catalyst. Particularly, among them, fibers have the advantages of large reaction area, low catalyst loss aimed the transmission, and high efficacy of optical transmission. For example, the doped TiO$_2$ was utilized to coated quartz fiber membranes in a photocatalytic reactor as shown in Fig. 10C, which driven out to have durable degradation ability with high efficiency. It is sensible to forecast that when g-C$_3$N$_4$ nanocomposite replaces TiO$_2$, they should accomplish similarly stable and high degradation performance for the contaminant evacuation. Though, the fiber reactor as well has its disadvantages such as being easily broken, expensive, and difficult to load the catalysts on the fiber[71]. As a result, distinctive sorts of photocatalytic reactors ought to be completely assessed when treating real wastewater of commercial scale utilizing g-C$_3$N$_4$.
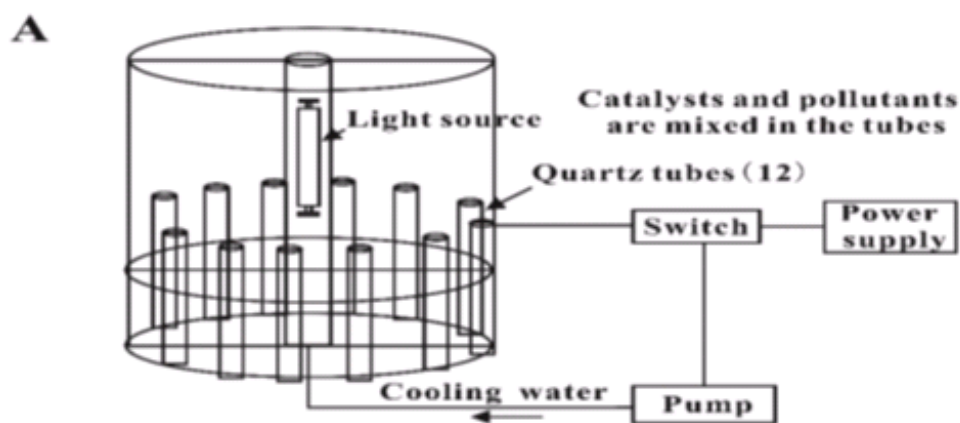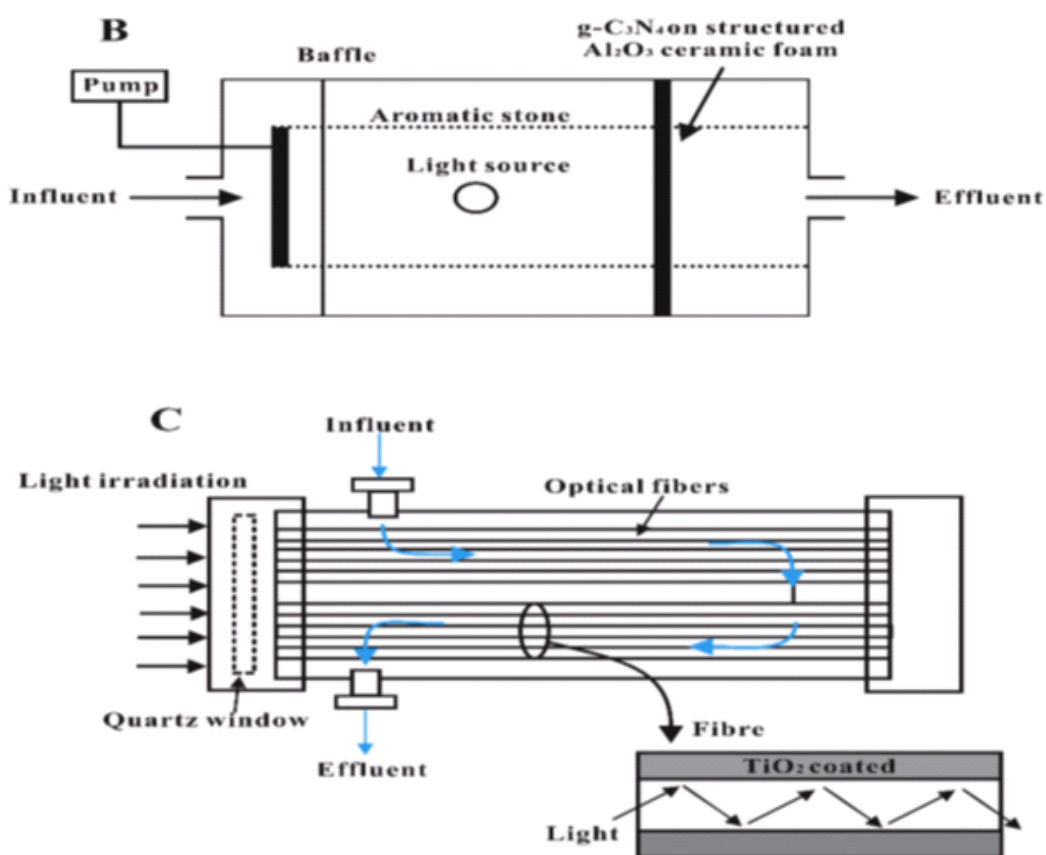
Fig.10. Different types of photocatalytic reactors for practical applications: (A) suspension photocatalytic reactor; (B) photocatalytic pool with g-C_3N_4 on structured Al_2O_3 ceramic foam; (C) catalyst coated optical fiber reactor.

5.3 Influence of environmental conditions on photocatalysis

Amid the photodegradation procedure, numerous ecological conditions, for example, pH of solution, reaction temperature, and broke down organic matters (DOM) assume noteworthy job for the photocatalytic execution which are not yet explored in the examination of g-C3N4 photocatalysis [76]. The solution pH impacts the ionization level of the chemical speciation. The oppositely charged contaminants and catalysts will advance the combination among them and along these increases the photodegradation adequacy. Moreover, the response temperature would seriously affect the photodegradation progress, as high temperature can quicken the redox response albeit too high temperature would change the nanostructure of the catalyst prompting potential catalyst deactivation [77].

Furthermore, DO assume an imperative job in debasing the contaminants. Moreover, DOM ordinarily exists in natural water and waste water and may pronouncedly effect on photochemical procedure due to the age of DOM-derived oxidative intermediates or their physicochemical extinguishing impacts. On one hand, DOM may cover the outside of the catalyst through adsorption, which prompts the less adsorption capacity of the catalyst and poor degradation effectiveness. Then again, DOM, for example, humid acid in the reaction blend can assimilate photons and produce active groups and consequently would decidedly influence the photo- oxidation rate [76]. These ecological conditions have been accounted to effects the catalytic capacity of TiO2. In this way, when another sort of g-C3N4 composites is integrated, pH, reaction temperature, DO, and DOM ought to be examined to determinate the best conditions for the photocatalytic execution [7, 46].

6. DISADVANTAGES OF g-C_3N_4 AS A PHOTOCATALYST

Besides its good catalytic activity, g-C_3N_4 is also inherited with a number of shortcomings that restricted its application as an efficient photocatalyst in water purification. The main drawbacks of g-C_3N_4 are (1) photoexcited EHP recombination (2) poor visible light absorption (3) low surface area and, (4) low quantum yield. Moreover, as discussed before, separation of g-C_3N_4 photocatalyst from reaction solution is very difficult, time consuming and involves wastage of

photocatalyst by centrifugation or filtration process. Various strategies to enhance photocatalytic activity such as (1) doping with metallic/non-metal elements, (2) coupling with other semiconductors, (3) manufacturing of the mesoporous structures, (4) co-polymerization and (5) magnetization by coupling with magnetic materials have been used[77].

To increase performance of g-C_3N_4 based nanocomposites, a few crucial necessities must be viewed as, for example, semiconductor light harvesting photocatalyst having narrow band gape for greatest absorption of solar energy favoring photogenerated EHP partition and encouraging transference of EHP[78]. Semiconductor photocatalyst must have appropriate redox potential for favored photochemical responses with an explanatory mechanism for strength of catalysts. In any case, satisfaction of every one of these prerequisites for a specific photocatalyst is difficult [80]. Nanocomposite photocatalyst have a few favorable circumstances, for example, (1)more absorption of light: semiconductors with limited band gape have more visible light absorptability to use and functionalize semiconductor photocatalyst with substantial band gapes: (2) viable photogenerated EHP partition and transference utilizing p-n junction or schottky junction development between metal/semiconductor heterojunction, (3) co-catalyst impact: assimilation with an appropriate co-catalysts can diminish redox potential at individual active sites: (4) stability achieved by shielding of active sites and functional groups on semiconductor surface through surface passivation [19].

Heterojunction development includes connection of mesoporous g-C_3N_4 (mpg-C_3N_4) having expanded internal surface area with characteristic properties of those activities as suitable host for semiconductor [82]. In this review, we are shortening different synthesize strategies for class of graphitic carbon nitride photocatalyst with its potential uses in waste water treatment [83]. Electronic structure and manufacture of g-C_3N_4 by various precursors have been talked about. The structuring and manufacture of various kinds of g-C_3N_4 based photocatalytic frameworks with different changes have been talked about with their job in waste water treatment [73]. The alterations incorporate nanocomposite with without metal, noble metals, non-metals and transportation, enhancing activity of catalyst and propagating charge transporter lifetime.

7. CONCLUSION

Fundamentally, this research was centered around the imperative difficulties stay in the development of g-C_3N_4 based complex nanocomposites with very much structured design. Detailed examination is expected to research the variations in electronic and lattice structure of g-C_3N_4 when coupled or doped with different semiconductors. The specialists working in ecological photocatalysis must concentrate on use of g-C_3N_4 based photocatalysts for oxidation or evacuation of unstable organic compounds and both indoor and open air decontamination. By heterojunction development with different non- metallic and metallic semiconductors, the reuse productivity and photocatalytic activity could be improved. Due to the appropriate band gape energy and great redox capacity of the photogenerated transporters, Graphitic carbon nitride has higher photocatalytic capacity than TiO_2 for the organic contaminants being examined. Component and intensifying doping is generally looked into, of which K doping is viable in advancing degrading efficacy with the k estimation of 0.0110min-1.

What's more, semiconductor doping likewise exhibits the capability of nearly high exploitation viability under irradiation of visible light, notably Z-scheme composite doping for example, Z-plot Ag_3PO_4-g-C_3N_4 which has indicated remarkable adequacy by degrading 100% MO inside 5 min with k value of 0.236 min-1. In all the different photoactive applications, noble nanoscale photocatalyst without metal frameworks dependent on g-C_3N_4 exhibited positive outcomes for its adaptable applications. Particularly, the great accomplishments in H_2 evaluation response outperforming that of with the Pt co-catalysts are exceptionally encouraging towards a maintainable generation of green and sustainable power source. Moreover, more endeavors ought to be dedicated to synthesize better functionalized yet minimal cost g-C_3N_4 composites to break down the obstinate natural contaminants with high and stable viability, to advance the business scale utilizations of photocatalysis.

ACKNOWLEDGEMENT

REFERENCES

[1] G. Zhang, S. Zang, L. Lin, Z.-A. Lan, G. Li, X. Wang, *ACS applied materials & interfaces* **2016**, *8*, 2287-2296.

[2] C. Tan, X. Cao, X.-J. Wu, Q. He, J. Yang, X. Zhang, J. Chen, W. Zhao, S. Han, G.-H. Nam, *Chemical reviews* **2017**, *117*, 6225-6331.

[3] A. Hajjaji, A. Atyaoui, K. Trabelsi, M. Amlouk, L. Bousselmi, B. Bessais, M. A. El Khakani, M. Gaidi, *American Journal of Analytical Chemistry* **2014**, *5*, 473.

[4] D. Bahnemann, *Solar energy* **2004**, *77*, 445-459.

[5] M. B. Ahmed, J. L. Zhou, H. H. Ngo, W. Guo, N. S. Thomaidis, J. Xu, *Journal of hazardous materials* **2017**, *323*, 274-298.

[6] S. Nayak, L. Mohapatra, K. Parida, *Journal of Materials Chemistry A* **2015**, *3*, 18622-18635.

[7] S. P. Adhikari, G. P. Awasthi, H. J. Kim, C. H. Park, C. S. Kim, *Langmuir* **2016**, *32*, 6163-6175.

[8] W.-J. Ong, L.-L. Tan, Y. H. Ng, S.-T. Yong, S.-P. Chai, *Chemical reviews* **2016**, *116*, 7159-7329.

[9] D. J. Klionsky, F. C. Abdalla, H. Abeliovich, R. T. Abraham, A. Acevedo-Arozena, K. Adeli, L. Agholme, M. Agnello, P. Agostinis, J. A. Aguirre-Ghiso, *Autophagy* **2012**, *8*, 445-544.

[10] J. Zhang, M. Zhang, C. Yang, X. Wang, *Advanced Materials* **2014**, *26*, 4121-4126.

[11] B. Zhu, J. Zhang, C. Jiang, B. Cheng, J. Yu, *Applied Catalysis B: Environmental* **2017**, *207*, 27-34.

[12] M. Zhou, Z. Hou, X. Chen, *Dalton Transactions* **2017**, *46*, 10641-10649.

[13] S. Yan, Z. Li, Z. Zou, *Langmuir* **2009**, *25*, 10397-10401.

[14] R. áNasir Baig, *Chemical Communications* **2015**, *51*, 15554-15557.

[15] M. Anpo, K. Chiba, M. Tomonari, S. Coluccia, M. Che, M. A. Fox, *Bulletin of the Chemical Society of Japan* **1991**, *64*, 543-551.

[16] Y. He, W. Chen, X. Li, Z. Zhang, J. Fu, C. Zhao, E. Xie, *ACS nano* **2012**, *7*, 174-182.

[17] B. Priya, P. Shandilya, P. Raizada, P. Thakur, N. Singh, P. Singh, *Journal of Molecular Catalysis A: Chemical* **2016**, *423*, 400-413.

[18] A. Fujishima, K. Honda, *nature* **1972**, *238*, 37.

[19] Q. Han, N. Chen, J. Zhang, L. Qu, *Materials Horizons* **2017**, *4*, 832-850.

[20] Q. Han, B. Wang, J. Gao, Z. Cheng, Y. Zhao, Z. Zhang, L. Qu, *ACS nano* **2016**, *10*, 2745-2751.

[21] W. Wang, J. C. Yu, D. Xia, P. K. Wong, Y. Li, *Environmental science & technology* **2013**, *47*, 8724-8732.

[22] L. Shi, L. Liang, F. Wang, M. Liu, S. Zhong, J. Sun, *Catalysis Communications* **2015**, *59*, 131-135.

[23] aZ. Zhu, Z. Lu, D. Wang, X. Tang, Y. Yan, W. Shi, Y. Wang, N. Gao, X. Yao, H. Dong, *Applied Catalysis B: Environmental* **2016**, *182*, 115-122; bQ. Liang, Z. Li, Z. H. Huang, F. Kang, Q. H. Yang, *Advanced Functional Materials* **2015**, *25*, 6885-6892.

[24] F. He, G. Chen, Y. Zhou, Y. Yu, L. Li, S. Hao, B. Liu, *Journal of Materials Chemistry A* **2016**, *4*, 3822-3827.

[25] B. Priya, P. Raizada, N. Singh, P. Thakur, P. Singh, *Journal of colloid and interface science* **2016**, *479*, 271-283.

[26] F. Li, X. Jiang, J. Zhao, S. Zhang, *Nano energy* **2015**, *16*, 488-515.

[27] Y. Wang, M. Qiao, J. Lv, G. Xu, Z. Zheng, X. Zhang, Y. Wu, *Fullerenes, Nanotubes and Carbon Nanostructures*

[28] B. Lin, C. Xue, X. Yan, G. Yang, G. Yang, B. Yang, *Applied Surface Science* **2015**, *357*, 346-355.

[29] S. Fang, Y. Xia, K. Lv, Q. Li, J. Sun, M. Li, *Applied Catalysis B: Environmental* **2016**, *185*, 225-232.

[30] Y. Xiang, S. Gong, Y. Zhao, X. Yin, J. Luo, K. Wu, Z.-H. Lu, C. Yang, *Journal of Materials Chemistry C* **2016**, *4*, 9998-10004.

[31] K. Zhu, Y. Du, J. Liu, X. Fan, Z. Duan, G. Song, A. Meng, Z. Li, Q. Li, *Journal of nanoscience and nanotechnology* **2017**, *17*, 2515-2519.

[32] D. J. Martin, K. Qiu, S. A. Shevlin, A. D. Handoko, X. Chen, Z. Guo, J. Tang, *Angewandte Chemie International Edition* **2014**, *53*, 9240-9245.

[33] L. Kong, Y. Dong, P. Jiang, G. Wang, H. Zhang, N. Zhao, *Journal of Materials Chemistry A* **2016**, *4*, 9998-10007.

[34] Z.-X. Li, F.-B. Shi, T. Zhang, H.-S. Wu, L.-D. Sun, C.-H. Yan, *Chemical Communications* **2011**, *47*, 8109-8111.

[35] H. Wang, X. Yuan, H. Wang, X. Chen, Z. Wu, L. Jiang, W. Xiong, G. Zeng, *Applied Catalysis B: Environmental* **2016**, *193*, 36-46.

[36] A. Zambon, J.-M. Mouesca, C. Gheorghiu, P. Bayle, J. Pécaut, M. Claeys-Bruno, S. Gambarelli, L. Dubois, *Chemical science* **2016**, *7*, 945-950.

[37] Y. Chen, W. Huang, D. He, Y. Situ, H. Huang, *ACS applied materials & interfaces* **2014**, *6*, 14405-14414.

[38] Y. Liu, X. Yuan, H. Wang, X. Chen, S. Gu, Q. Jiang, Z. Wu, L. Jiang, Y. Wu, G. Zeng, *Catalysis Communications* **2015**, *70*, 17-20.

[39] R. C. Pawar, S. Kang, S. H. Ahn, C. S. Lee, *Rsc Advances* **2015**, *5*, 24281-24292.

[40] J. Wen, J. Xie, X. Chen, X. Li, *Applied Surface Science* **2017**, *391*, 72-123.

[41] X. Chen, J. Wei, R. Hou, Y. Liang, Z. Xie, Y. Zhu, X. Zhang, H. Wang, *Applied Catalysis B: Environmental* **2016**, *188*, 342-350.

[42] Y. Lu, D. Chu, M. Zhu, Y. Du, P. Yang, *Physical Chemistry Chemical Physics* **2015**, *17*, 17355-17361.

[43] Y. Dong, D. Wang, H. Zhang, Y. Chen, W. Liu, Y. Wang, *Materials Letters* **2017**, *196*, 100-103.

[44] J. Fu, Y. Tian, B. Chang, F. Xi, X. Dong, *Journal of Materials Chemistry* **2012**, *22*, 21159-21166.

[45] J. Hong, Y. Wang, Y. Wang, W. Zhang, R. Xu, *ChemSusChem* **2013**, *6*, 2263-2268.

[46] S.-W. Cao, X.-F. Liu, Y.-P. Yuan, Z.-Y. Zhang, J. Fang, S. C. J. Loo, J. Barber, T. C. Sum, C. Xue, *Physical Chemistry Chemical Physics* **2013**, *15*, 18363-18366.

[47] S.-W. Cao, Y.-P. Yuan, J. Barber, S. C. J. Loo, C. Xue, *Applied Surface Science* **2014**, *319*, 344-349.

[48] D. Wang, J. Pan, H. Li, J. Liu, Y. Wang, L. Kang, J. Yao, *Journal of Materials Chemistry A* **2016**, *4*, 290-296.

[49] X. Wang, J. Chen, X. Guan, L. Guo, *international journal of hydrogen energy* **2015**, *40*, 7546-7552.

[50] Y. Cui, Z. Ding, X. Fu, X. Wang, *Angewandte Chemie* **2012**, *124*, 11984-11988.

[51] J. Liu, Y. Liu, N. Liu, Y. Han, X. Zhang, H. Huang, Y. Lifshitz, S.-T. Lee, J. Zhong, Z. Kang, *Science* **2015**, *347*, 970-974.

[52] A. Akhundi, A. Habibi-Yangjeh, *Rsc Advances* **2016**, *6*, 106572-106583.

[53] G. Dong, K. Zhao, L. Zhang, *Chemical Communications* **2012**, *48*, 6178-6180.

[54] G. Dong, Y. Zhang, Q. Pan, J. Qiu, *Journal of Photochemistry and Photobiology C: Photochemistry Reviews* **2014**, *20*, 33-50.

[55] F. Dong, Z. Wang, Y. Li, W.-K. Ho, S. Lee, *Environmental science & technology* **2014**, *48*, 10345-10353.

[56] C. Dai, Y. Zhou, H. Peng, S. Huang, P. Qin, J. Zhang, Y. Yang, L. Luo, X. Zhang, *Journal of industrial and engineering chemistry* **2018**, *62*, 106-119.

[57] J. Barzegar, A. Habibi-Yangjeh, M. Mousavi, *Solid State Sciences* **2018**, *77*, 62-73.

[58] B. Pare, P. Singh, S. Jonnalagadda, **2008**.

[59] Y. Hou, A. B. Laursen, J. Zhang, G. Zhang, Y. Zhu, X. Wang, S. Dahl, I. Chorkendorff, *Angewandte Chemie* **2013**, *125*, 3709-3713.

[60] X. Xia, N. Deng, G. Cui, J. Xie, X. Shi, Y. Zhao, Q. Wang, W. Wang, B. Tang, *Chemical Communications* **2015**, *51*, 10899-10902.

[61] S. Ma, S. Zhan, Y. Jia, Q. Shi, Q. Zhou, *Applied Catalysis B: Environmental* **2016**, *186*, 77-87.

[62] S. Malato, J. Blanco, A. Vidal, C. Richter, *Applied Catalysis B: Environmental* **2002**, *37*, 1-15.

[63] G. Mamba, A. Mishra, *Applied Catalysis B: Environmental* **2016**, *198*, 347-377.

[64] P. Niu, L. Zhang, G. Liu, H. M. Cheng, *Advanced Functional Materials* **2012**, *22*, 4763-4770.

[65] U. Pagga, D. Brown, *Chemosphere* **1986**, *15*, 479-491.

[66] S. Patnaik, S. Martha, S. Acharya, K. Parida, *Inorganic Chemistry Frontiers* **2016**, *3*, 336-347.

[67] S. Hu, F. Li, Z. Fan, F. Wang, Y. Zhao, Z. Lv, *Dalton Transactions* **2015**, *44*, 1084-1092.

[68] R. Janssens, M. K. Mandal, K. K. Dubey, P. Luis, *Science of the Total Environment* **2017**, *599*, 612-626.

[69] D. Jiang, J. Li, C. Xing, Z. Zhang, S. Meng, M. Chen, *ACS applied materials & interfaces* **2015**, *7*, 19234-19242.

[70] Y. Jiang, P. Liu, Y. Liu, X. Liu, F. Li, L. Ni, Y. Yan, P. Huo, *Separation and Purification Technology* **2016**, *170*, 10-21.

[71] K. Xie, N. Umezawa, N. Zhang, P. Reunchan, Y. Zhang, J. Ye, *Energy & Environmental Science* **2011**, *4*, 4211-4219.

[72] H.-Y. He, *Particulate Science and Technology* **2017**, *35*, 410-417.

[73] M. Hatat-Fraile, R. Liang, M. J. Arlos, R. X. He, P. Peng, M. R. Servos, Y. N. Zhou, *Chemical Engineering Journal* **2017**, *330*, 531-540.

[74] M.-H. Wu, B.-T. Xu, G. Xu, M.-N. Wang, J. Ma, C.-Y. Pan, R. Sun, T. Han, L. Tang, *Environmental geochemistry and health* **2017**, *39*, 729-738.

[75] P. Raizada, P. Shandilya, P. Singh, P. Thakur, *Journal of Taibah University for Science* **2017**, *11*, 689-699.

[76] L. Ye, D. Wang, S. Chen, *ACS applied materials & interfaces* **2016**, *8*, 5280-5289.